



Performance Analysis of Bi-directional Improved Hybrid Three Quasi Z source Converter

R. Alla*, A. Chowdhury

Department of Electrical Engineering, Sardar Vallabhbhai National Institute of Technology, Surat, India

PAPER INFO

Paper history:

Received 19 November 2022

Received in revised form 08 March 2023

Accepted 20 March 20, 2023

Keywords:

Z source Converter

Shoot-through Duty Ratio

Voltage Gain

Predictive Control

ABSTRACT

Bi-directional power converters are utilized for effective management of available electrical energy associated with renewable energy systems with the use of an energy storage system. Improved hybrid three quasi z source converter (IHTQZSC) is proposed in this paper which has been providing a higher voltage gain without any switched capacitor or charge pump cells. IHTQZSC has been intended for bi-directional power transfer and control applications in this paper. The converter ensures a widespread voltage gain in a single stage DC↔AC power conversion system with lesser shoot-through time instants. The competence of the converter is acclaimed with voltage stress, current stress, peak switching device power and power losses compared with the other high voltage gain converters. Impact of voltage gain and power drawn by the converter on the efficiency has been explained. The four-quadrant power control is achieved with the constant switching frequency predictive controller. The DC-link voltage of the converter is controlled with a PI controller, and a predictive controller is used for the grid current tracking. The bi-directional working of the converter is illustrated with MATLAB/Simulink software

doi: 10.5829/ije.2023.36.07a.06

1. INTRODUCTION

Recent developments in the fields of renewable energy extraction, electric vehicles (EVs) and energy storage systems (ESS) are associated with an efficient power electronic interface (PEI). PEI plays a critical role in DC-DC, DC-AC, AC-AC and AC-DC power conversion systems either by step-up or step-down the voltage and allowing uni-directional or bi-directional power transfer. High gain DC-DC converter along with 9 level multilevel inverter is used for interfacing hybrid energy system to the utility [1]. An interleaved DC-DC converter has been designed to reduce voltage stress and providing higher voltage gain compared with a conventional boost converter [2]. The diode bridge rectifier (DBR) is used along with a further stage of DC-DC converter in uni-directional AC-DC power conversion [3, 4]. A voltage source converter (VSC) is used on behalf of DBR for AC-DC power conversion, popularly known as a PWM rectifier, which can improve the power quality on the source side and allows bi-directional power transferring

[5-8]. So far, the different PEI discussed are of two-stage power conversion systems. A DBR or a VSC facilitates in rectification stage and a DC-DC converter is accustomed to either step-up or step-down the dc voltage [9]. Bi-directional PEI is preferred over uni-directional PEI, particularly in EVs and ESS, as it reduces the cost and volume of the system. Furthermore, AC-DC bi-directional PEI is capable of maintaining an active and reactive power balance in the system.

Impedance source converters (ISC) are providing higher voltage gain in a single-stage power conversion system. Shoot-through phenomena in VSC are avoided with the introduction of dead time in between switching devices on the same leg. Dead-time is no need to provide among the switches of the same leg in ISC. Shoot-through states (STS) are intended for voltage boost functionality in ISC, whereas STS are avoided in VSC. These shortcomings in VSC are overcome with the ISC, which can use the STS to boost the input voltage while the power is transferring to the loads in normal switching states. The family of ISC is developed based on the

* Corresponding Author Email: ramanjaneyualla@gmail.com
(R. Alla)

operating principle of the basic z source converter (ZSC) [10]. Quasi Z source converter (QZSC) inherits the features of ZSC without any change in voltage gain, developed to provide a common DC-rail with reduced capacitor stress [11].

Further, different ISC are developed to meet high voltage gain, reduced voltage and current stresses [12-16]. QZSC is facilitated as a bi-directional DC-DC converter [17]. Battery assisted ZSC with an ultra-capacitor as an input source is worked as a bi-directional converter for electric drive applications [18]. All regions of locomotive operation are discussed with bi-directional ZSC [19]. The working of ISC depends on the insertion of STS along with the conventional switching states. The pulse width modulation (PWM) methods are developed to include STS along with non shoot-through switching states (nSTS) for the voltage buck-boost action of ISC, among which simple boost control (SBC) method is eminently implemented in most of the applications [20]. The DC-link voltage of the ISC are regulated along with the inductor current ripples with a dual-loop control method, requires two PI controllers [21]. ISC has been developed with switched capacitor or charge pump based configuration. It has been identified that atleast a capacitor is carrying a load current in these converters, which can increase the rating of the capacitor such that size and cost of the converters has been increased [22-25]. MPC is a very attractive control method that can be implemented for most power electronic applications. PI controllers are not needed with the MPC. Direct MPC has been changed to working at a constant switching frequency in a grid-connected IHTQZC [26]. The comparison of traditional VSC and ZSC is carried out in fuel cell applications [27].

Significant research has to be enforced to analyze the performance of high voltage gain bi-directional ISC in various applications. Low voltage gain ZSC and QZSC are assigned in most of the applications so far developed. This paper elaborates on the ability of high voltage gain IHTQZSC among other ISC by considering the details about the voltage and current stresses, pea switching device power and power losses that occurred in the converters. This paper addresses bi-directional power conversion working of IHTQZSC. Instead of two PI controllers [20] for DC-link voltage regulation, a single PI controller is addressed in this paper. The grid current of the converter is controlled with a predictive controller (PC), which accomplishes a constant switching frequency. Section 2 of the article explains the bi-directional IHTQZSC configuration and working. Voltage gain, voltage stress, current stresses and power losses in the impedance network of high voltage gain ISC are presented in section 3. DC-link voltage control and grid current control are discussed in section 4. The performance of the converter providing reactive power support to the grid and the bi-directional power flow

capability is illustrated with the SimPower System tool in MATLAB software, in section 5 of this paper.

2. MATHEMATICAL MODEL OF IHTQZSC

Impedance network consists inductors (L_1, L_2, L_3 and L_4), capacitors (C_1, C_2, C_3, C_4, C_5 and C_6) and bi-directional switches (S_1, S_2 and S_3) inserted in between dc source and the VSC. The configuration of the bi-directional IHTQZSC is shown in Figure 1. Switches are introduced in place of diodes of [27], for allowing bi-directional power. For a VSC, the relation between peak AC voltage (v_{peak}) and the DC-link voltage (V_{DC}) is expressed in Equation (1):

$$v_{peak} = M \frac{V_{DC}}{2} \tag{1}$$

where M is modulation index.

The converter steps-up the input voltage of the battery (V_{Bat}) for maintaining the required DC-link voltage V_{DC} at PWM inverter and feeding power into the grid. Similarly, the converter steps-down the voltage V_{DC} at the PWM rectifier to meet V_{Bat} and feeding the power into the DC source. Therefore, the converter operation is explained firstly as a PWM inverter with input voltage boost mode, and secondly, PWM rectifier with voltage buck mode.

2. 1. STS Operation of IHTQZSC as PWM Inverter with Voltage Boost

The voltage boost operation is achieved with the insertion of STS in addition to nSTS. The converter undergoes shoot-through, at a time duration of $d_{ST}T$ for a switching cycle of time period T, so that the switches in the three legs are turned on simultaneously and it causes $V_{DC}=0$. Hence the zero power, i.e., $P_{Grid}=0$ transfers to the grid represented with dashed lines shown in Figure 2.

Here d_{ST} is the shoot-through duty ratio. The switches S_1, S_2 and S_3 in the converter are turned off in this mode. It allows capacitors to discharge energy into the inductors. The voltage across the inductors, switches,

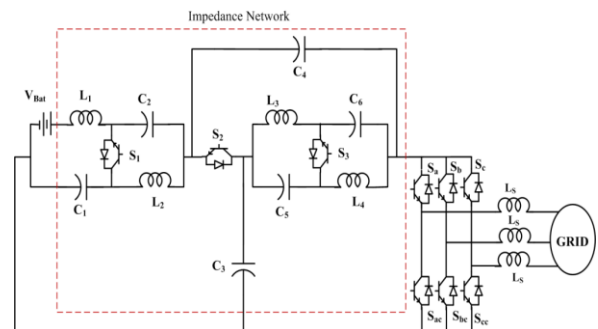


Figure 1. Circuit Diagram of IHTQZSC

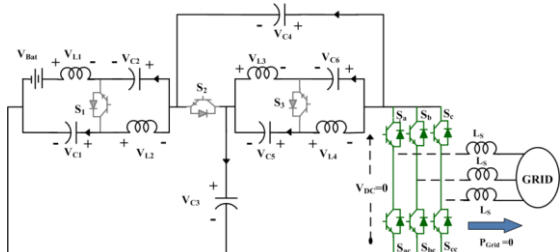


Figure 2. IHTQZSC as PWM inverter in STS

current through the diodes and capacitors are expressed in Equations (2) to (8):

$$v_{L1} = v_{C2} + v_{C4} + V_{Bat}; v_{L2} = v_{C1} + v_{C4} \quad (2)$$

$$v_{L3} = v_{C3} + v_{C6}; v_{L4} = v_{C3} + v_{C5} \quad (3)$$

$$v_{S1} = v_{C1} + v_{C2} + v_{C4}; v_{S2} = v_{C3} + v_{C4} \quad (4)$$

$$v_{S3} = v_{C3} + v_{C5} + v_{C6} \quad (5)$$

$$i_{C1} = -i_{L2}; i_{C2} = -i_{L1}; i_{S1} = i_{S2} = i_{S3} = 0 \quad (6)$$

$$i_{C3} = -(i_{L3} + i_{L4}); i_{C4} = -(i_{L1} + i_{L2}) \quad (7)$$

$$i_{C5} = -i_{L3}; i_{C6} = -i_{L4} \quad (8)$$

2. 2. nSTS operation of IHTQZSC as PWM Inverter with Voltage Boost

General sinusoidal pulse width modulated (SPWM) signals are sent to the switches in the three legs of the converter at a time duration of $(1-d_{ST})T$. The switches S_1, S_2 and S_3 in the converter are turned on to allow charging of the capacitors as shown in Figure 3.

In nSTS mode, the energy from the dc source is fed into the grid. Every switch in the converter has a duty ratio of $(1-d_{ST})$ in nSTS mode. The voltage across the inductors, diodes, current through the switches and capacitors are expressed in Equations (9) to (16):

$$v_{L1} = -v_{C1} + v_{Bat}; v_{L2} = -v_{C2}; \quad (9)$$

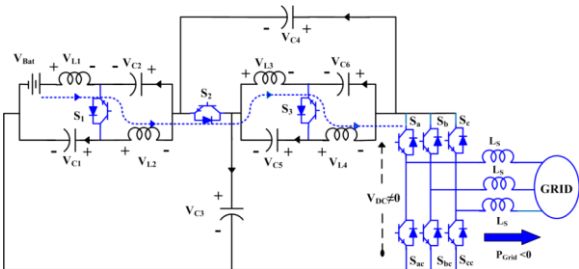


Figure 3. IHTQZSC as PWM inverter in nSTS

$$v_{L3} = -v_{C5}; v_{L4} = -v_{C6}; v_{DC} = v_{C3} + v_{C4} \quad (10)$$

$$v_{S1} = v_{S2} = v_{S3} = 0 \quad (11)$$

$$i_{L1} + i_{C2} = i_{L2} + i_{C1} = i_{S1} \quad (12)$$

$$i_{L3} + i_{C6} = i_{L4} + i_{C5} = i_{S3} \quad (13)$$

$$i_{L2} + i_{C4} - i_{C2} = i_{L3} + i_{C3} - i_{C5} = i_{S2} \quad (14)$$

$$i_{C4} + i_{C6} = i_{L4} - i_{Con}; \quad (15)$$

$$i_{Con} = S_a i_a + S_b i_b + S_c i_c \quad (16)$$

According to the volt-s and ampere-s balance principle the steady state voltage across capacitors and current through the inductors are expressed in Equations (17) to (23). Equation (1) has been expressed in terms of G in Equation (22). For a SBC [20], $M=1-d_{ST}$. Here I_{Con} is the average current through the converter terminals and R_L is the equivalent resistance about the power injected into the grid.

$$V_{C1} = \frac{1 - 3d_{ST}}{(1 - 4d_{ST})} V_{Bat} \quad (17)$$

$$V_{C2} = V_{C5} = V_{C6} = \frac{d_{ST}}{(1 - 4d_{ST})} V_{Bat} \quad (18)$$

$$V_{C4} = \frac{2d_{ST}}{(1 - 4d_{ST})} V_{Bat} \quad (19)$$

$$V_{C3} = \frac{1 - d_{ST}}{(1 - 4d_{ST})} V_{Bat} \quad (20)$$

$$V_{DC} = \frac{1}{(1 - 4d_{ST})} V_{Bat}; B_{ST} = \frac{1}{(1 - 4d_{ST})} \quad (21)$$

$$v_{peak} = G \frac{V_{DC}}{2}; G = MB_{ST} \quad (22)$$

$$I_{L1} = \frac{1 - d_{ST}}{(1 - 4d_{ST})} I_{Con}; I_{Con} = \frac{(1 - d_{ST})V_{DC}}{R_L} \quad (23)$$

$$I_{L1} = I_{L2} = I_{L3} = I_{L4}$$

2. 3. STS Operation of IHTQZSC as PWM Rectifier with Voltage Buck Action

The VSC acts as a PWM rectifier. The DC-link voltage V_{DC} is stepped down to meet the battery voltage V_{Bat} with power flowing from the grid to the battery. Reverse phenomena occur here, in comparison with section 2.1. Thereby the voltage across

the inductors and current through the capacitors are expressed with a negative sign compared with the equations represented in section 2.1. The insertion of STS provides voltage buck action. Figure 4 illustrates the STS operation of the converter, at a time duration of $d_{CK}T$, makes the switches in the three legs are turned on simultaneously, causes $V_{DC}=0$ and hence the zero power, i.e., $P_{Grid}=0$ transfers to the battery from the grid represented with dashed lines. The switches S_1 , S_2 and S_3 in the converter are turned off in this mode, allows the inductors to charge the capacitors.

2. 4. nSTS Operation of IHTQZSC as PWM Rectifier with Voltage Buck Action

Similar to section 2.2, switches S_1 , S_2 and S_3 in the converter are turned on, the energy from the grid is fed into the battery as well as the capacitors are discharging shown in Figure 5. Every switch in the converter has a duty ratio of $(1-d_{CK})$. The voltage across the inductors and current through the capacitors are expressed with negative sign. The steady state voltage across capacitors, dc-link voltage and inductor currents are expressed in Equations (24) to (30). Here I_{Bat} is the current drawn by the DC source. Both PWM inverter working and PWM rectifier working are accomplished with the insertion of STS for a time interval of $d_{ST}T$ or $d_{CK}T$. Based on Equations (21) and (29), $d_{ST}=d_{CK}$.

3. PARAMETER DESIGN OF IHTQZSC

Voltage stress and current stress of every component in the configuration of the IHTQZSC are deduced for the

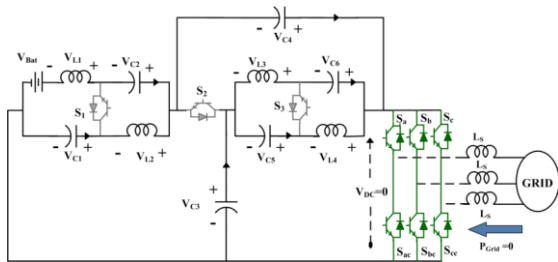


Figure 4. IHTQZSC as PWM Rectifier in STS operation

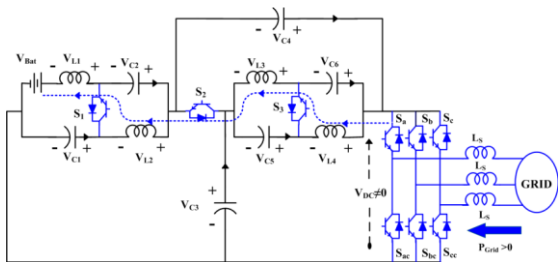


Figure 5. IHTQZSC as PWM Rectifier in nSTS operation

design of active and passive components. The voltage and current stresses are equal in the converter while working as a PWM inverter or PWM rectifier since the shoot-through duty ratio values are equal. The values of capacitances expressed in Equations (31) and (32) are selected based on their voltage stress, which is maximum in STS. Hence the Equations (6) to (8) are considered for capacitance calculation by allowing a ripple percentage of r_v in capacitor voltage.

$$V_{C1} = (1 - 3d_{CK})V_{DC} \tag{24}$$

$$V_{C2} = V_{C5} = V_{C6} = d_{CK}V_{DC} \tag{25}$$

$$V_{C3} = (1 - 2d_{CK})V_{DC} \tag{26}$$

$$V_{C4} = 2d_{CK}V_{DC} \tag{27}$$

$$V_{Bat} = (1 - 4d_{CK})V_{DC} \tag{28}$$

$$V_{Bat} = B_{CK}V_{DC} ; B_{CK} = (1 - 4d_{CK}) \tag{29}$$

$$I_{L1} = I_{L2} = I_{L3} = I_{L4} = I_{Bat} = \frac{1 - d_{CK}}{(1 - 4d_{CK})} I_{Con} \tag{30}$$

The current stress through the inductors is maximum in STS, hence Equations (2) and (3) are chosen for evaluating the inductance value by allowing a percentage current ripple of r_i . Inductance value is expressed in Equation (33). Voltage stress across the switches and current stress in the switches are expressed in Equation (34).

$$C_1 = \frac{d_{ST}(1 - 4d_{ST})I_{Bat}}{r_v(1 - 3d_{ST})V_{Bat}f_s} \tag{31}$$

$$C_2 = C_5 = C_6 = \frac{(1 - 4d_{ST})I_{Bat}}{r_vV_{Bat}f_s}$$

$$C_3 = \frac{d_{ST}(1 - 4d_{ST})I_{Bat}}{r_v(1 - 2d_{ST})V_{Bat}f_s} \tag{32}$$

$$C_4 = \frac{0.5(1 - 4d_{ST})I_{Bat}}{r_vV_{Bat}f_s}$$

$$L_1 = L_2 = L_3 = L_4 = \frac{d_{ST}(1 - d_{ST})V_{Bat}}{r_i(1 - 4d_{ST})I_{Bat}f_s} \tag{33}$$

$$\begin{aligned} V_{S1} &= V_{S2} = V_{S3} = V_{DC} \\ V_{Sa} &= V_{Sb} = V_{Sc} = V_{Saa} = V_{Sbb} = V_{Scc} = V_{DC} \\ I_{S1} &= I_{S2} = I_{S3} = B_{ST}I_{Con} \end{aligned} \tag{34}$$

$$I_{Sa} = I_{Sb} = V_{Sc} = I_{Saa} = I_{Sbb} = I_{Scc} = \frac{4I_{Bat}}{3}$$

$$i_{ST} = I_{L1} + I_{L2} + I_{L3} + I_{L4} \quad (35)$$

$$i_{Sa} = \frac{1}{2}i_a + \frac{i_{ST}}{3} \quad (36)$$

$$i_{peak} = \frac{4P_{Grid}}{3V_{Bat}M \cos \varphi} \quad (37)$$

The product of voltage and current stress provides peak switching device power (SDP) of the converter. Shoot-through current and switch S_a current through the switches in the converter legs [28] is expressed in Equations (35) and (36). i_{Sa} has a maximum value when i_a is at its peak value, expressed in Equation (37). The current through switch S_a has a peak current of either i_{Sa} or i_{peak} . Total SDP of IHTQZSC is sum of the SDP of the switches in the converter and expressed in Equation (38):

$$SDP = V_{S1}I_{S1} + V_{S2}I_{S2} + V_{S3}I_{S3} + 6V_{DC} \max\{i_{Sa} \text{ or } i_{peak}\} \quad (38)$$

3. 1. Power Losses The total power losses in the impedance network are due to the losses in inductors, capacitors and switches. Power loss in the inductors and capacitors are given in Equations (39) and (40). r_{ind} , r_{cap} and r_d are the internal resistances of the inductors, capacitors and the switches. t_{on} and t_{off} are the turn on and turn off transition times of the switches at a switching frequency of f_s . The Ohmic losses and switching losses in the impedance network and converter legs are expressed in Equations (41) and (44).

$$P_{ind} = 4(1 - d_{ST})^2 B_{ST}^2 I_{Con}^2 r_{ind} \quad (39)$$

$$P_{Cap} = 12I_{Bat}^2 \frac{d_{ST}}{(1 - d_{ST})} r_{cap} \quad (40)$$

$$P_{Nw-ohm} = (I_{S1rms}^2 + I_{S2rms}^2 + I_{S3rms}^2)r_D \quad (41)$$

$$P_{Nw-turn} = (V_{S1}I_{S1} + V_{S2}I_{S2} + V_{S3}I_{S3}) \frac{t_{on} + t_{off}}{2} f_s \quad (42)$$

$$I_{inv-sw,rms} = \sqrt{\frac{16}{9} d_{ST} I_{L1}^2 + \frac{16}{9} \frac{P_{Grid}^2 (1 - d_{ST})}{G^2 V_{Bat}^2 \cos^2 \varphi}} \quad (43)$$

3. 2. Comparative Analysis with other High Voltage Gain ISC

The voltage boost factor (B_{ST}), maximum voltage and current stress in the converter elements and peak SDP are preferred for the identification of the competence of IHTQZSC with another high voltage gain ISC. It has been noticed that IHTQZSC provides a wider voltage gain compared with other higher voltage gain ISC with a lower shoot-through duty ratio has shown in Figure 6(a). The maximum value of the capacitor voltage stress of IHTQZSC is lower than the voltage stress reported in literature [14, 15] at higher voltage gain requirements. Except Zhu et al. [12] reported that the remaining converters have an equal amount of maximum inductor current stress listed in Table 1. IHTQZSC has a lower switch current stress compared with current stress in the switches reported by Jagan et al. [14] and Zhu et al. [15]. The proposed converter has a lower value of maximum voltage stress in the switches of the impedance network. IHTQZSC has a nearer SDP value considered by Jagan et al. [14] and Zhu et al. [15] are shown in Figure 6(b).

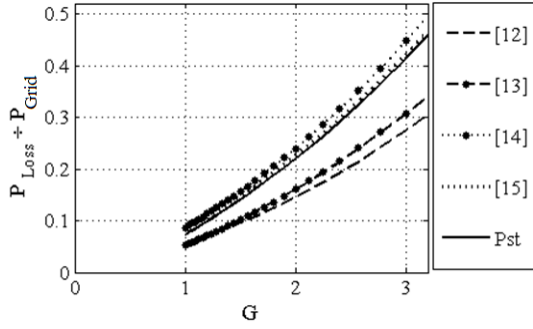
$$P_{inv-sw} = 6 \left\{ \frac{16}{9} d_{ST} I_{Bat}^2 + \frac{16}{9} \frac{P_{Grid}^2 (1 - d_{ST})}{G^2 V_{Bat}^2 \cos^2 \varphi} \right\} r_d \quad (44)$$

$$P_{inv-turn} = 6V_{DC} \frac{I_{ST}}{3} \frac{t_{on} + t_{off}}{2} f_s \quad (45)$$

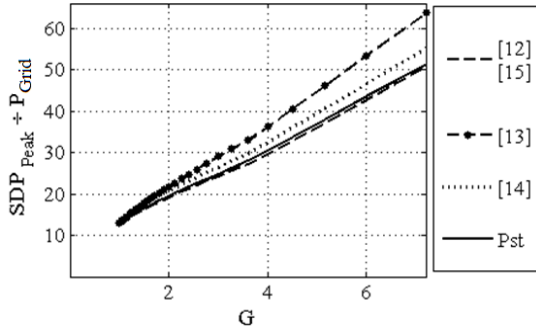
TABLE 1. Voltage and Current Stress of IHTQZSC

	[12]	[13]	[14]	[15]	Pst - IHTQZSC
$\frac{V_{CMax}}{V_{Bat}}$	$B_{ST}(1 - d_{ST}) / (1 + d_{ST})$	B_{ST}	$d_{ST}(2 - d_{ST})B_{ST}$	$d_{ST}(3 - 2d_{ST})B_{ST}$	$(1 - 2d_{ST})B_{ST}$
$\frac{I_{LMax}}{I_{Con}}$	$B_{ST}(1 - d_{ST}) / (1 + d_{ST})$	$(1 - d_{ST})B_{ST}$	$(1 - d_{ST})B_{ST}$	$(1 - d_{ST})B_{ST}$	$(1 - d_{ST})B_{ST}$
$\frac{I_{SMax}}{I_{Con}}$	B_{ST}	$(1 - d_{ST})B_{ST}$	B_{ST}	B_{ST}	B_{ST}
$\frac{V_{SMax}}{V_{Bat}}$	B_{ST}	B_{ST}	B_{ST}	B_{ST}	B_{ST}
	$B_{ST}(1 - d_{ST}) / (1 + d_{ST})$	$d_{ST}B_{ST}$	$d_{ST}B_{ST}$	$d_{ST}B_{ST}$	B_{ST}
	$B_{ST}d_{ST} / (1 + d_{ST})$	$(1 - d_{ST})B_{ST}$	$(1 - d_{ST})B_{ST}$	$(1 - d_{ST})B_{ST}$	

V_{SMAX} , V_{CMAX} Maximum voltage in switch and capacitors; I_{LMAX} , I_{LMAX} Maximum current through switches and inductors



(a)



(b)

Figure 6. (a) Power loss variation with G (b) SDP variation with G

The converters reported by Jagan et al. [14], Zhu et al. [15] and IHTQZSC are having very nearer voltage gain and an equal amount of inductor maximum current stress. The maximum current stress and voltage stress in the switches of IHTQZSC are lower than other converters. IHTQZSC has lower SDP compared with reported data by Nozadian et al. [13] Jagan et al. [14] and has a very nearer SDP value compared with data reported by Zhu et al. [12] and Zhu et al. [15]. Hence the power losses are considered for highlighting the significance of IHTQZSC, plotted in Figure 6(a). It has been verified that IHTQZSC has a lower power loss compared to data reported by Jagan et al. [14] and Zhu et al. [15] among high voltage gain non-coupled ISC.

4. CONTROL METHOD

CSF-PC controller is utilizing for the controlling of IHTQZSC [27] as shown in Figure 7. The converter has been controlled on DC-side of the converter to attain a constant DC-link voltage V_{DC} . But V_{DC} has been varying from zero to a peak value. Hence it can be challenging to control direct V_{DC} . That's why V_{DC} has been expressed as a sum of V_{C3} and V_{C4} . The DC-link voltage V_{DC} is regulated with a PI controller. The bode diagram in dotted line shown in Figure 11 represents a negative gain margin and phase margin due to RHP zero makes the

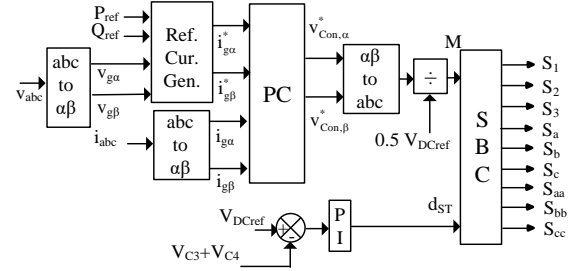


Figure 7. Grid-Tied IHTQZSC with CSF-PC

uncompensated system becomes unstable. With the proper selection of parameters $k_p=0.0003$ and $k_i=0.02$ in PI controller, bode diagram for the compensated system represented in solid line in Figure 7 exhibits system stability.

PC is implemented for grid current tracking by predicting the two orthogonal voltage vectors. Here R_S is considered for the filter resistance and V_{Con} is the voltage across the converter. v_{abc} and i_{abc} are grid voltage and currents. The grid current equation is expressed in Equation (46). The predicted grid current during a sampling time of T_s with Euler's approximation is represented in $\alpha\beta$ reference frame in Equation (47).

$$L_S \frac{di_{abc}}{dt} = -R_S i_{abc} + v_{Con} - v_{abc} \quad (46)$$

$$i_{g\alpha\beta}(k+1) = \left(1 - \frac{R_S T_s}{L_S}\right) i_{g\alpha\beta}(k) + \frac{T_s}{L_S} (v_{Con,\alpha\beta}(k) - v_{g\alpha\beta}(k)) \quad (47)$$

$$C = C_\alpha + C_\beta$$

$$C_\alpha = \left(\left| i_{g\alpha}^*(k+1) - i_{g\alpha}(k+1) \right| \right)^2; \quad (48)$$

$$C_\beta = \left(\left| i_{g\beta}^*(k+1) - i_{g\beta}(k+1) \right| \right)^2$$

$$i_{g\alpha}^* = \frac{2}{3} (P_{ref} v_{g\alpha} + Q_{ref} v_{g\beta}) \quad (49)$$

$$i_{g\beta}^* = \frac{2}{3} (P_{ref} v_{g\beta} - Q_{ref} v_{g\alpha}) \quad (50)$$

The quadratic cost function is defined for identifying the optimal switching vectors mentioned in Equation (48). $i_{g\alpha}^*$ and $i_{g\beta}^*$ are the reference values of grid current, evaluated by considering the required amount of active and reactive powers P_{ref} and Q_{ref} injected or consumed from the grid, respectively. The predicted orthogonal voltage vectors $v_{Con,\alpha}^*$ and $v_{Con,\beta}^*$ are obtained with the maxima-minima concept represented in Equation (51).

$$\begin{aligned}
 v_{Con,\alpha}^* &= -\frac{L_S}{T_S} A; A = \left(1 - \frac{R_S T_S}{L_S}\right) i_{g\alpha}(k) + \frac{T_S}{L_S} v_{g\alpha}(k) - i_{g\alpha}^*(k+1) \\
 v_{Con,\beta}^* &= -\frac{L_S}{T_S} B; B = \left(1 - \frac{R_S T_S}{L_S}\right) i_{g\beta}(k) + \frac{T_S}{L_S} v_{g\beta}(k) - i_{g\beta}^*(k+1)
 \end{aligned}
 \tag{51}$$

V_{DC} has been controlled with PI controller by generating d_{ST} and the four-quadrant operation of power is controlled with the implementation of PC for grid current tracking by generating $v_{Con,\alpha}^*$ and $v_{Con,\beta}^*$. These optimal voltage vectors send the modulating signals to the SBC along with d_{ST} from the PI controller. Constant switching frequency is obtained with the use of a modulator in the SBC controller, operates the converter in STS and nSTS mode.

5. RESULTS AND DISCUSSION

Performance of IHTQZSC has been analysed during the four-quadrant power control with MATLAB Simulink results. The direction of i_{abc} is considered positive when the converter acts as PWM rectifier feeding power into the DC source. The system parameters are - Inductance 1mH, Capacitance 470µf, switching frequency 10kHz, grid voltage 220Vrms, grid inductance 15mH, input voltage 200V and sampling time of 25µs.

Active power (P) and reactive power (Q) along with i_{abc} and v_{abc} are chosen grid side parameters for the identification of the converter response. V_{Bat} , V_{C3} , V_{DC} and inductor current or DC source current I_{L1} are considered as DC side parameters.

QI, QII, QIII and QIV are quadrants

Figure 8 shows the response of the converter while operating in Q_I, consumes P of 1000W at unity power factor (upf) up to 0.4s and afterward absorbs Q of 1000VAr. It means the converter acts as a PWM rectifier and provides VAr support to the grid. Hence the peak of i_{abc} has been changed to 5.23A from 3.7A. The controller affords a quick response from the converter with a change in Q. The converter draws a DC source current of 5A at V_{Bat} of 200V and maintaining V_{C3} at and 306.6V, V_{DC} at 413V. The converter shifts its operation from Q_I to Q_{IV} at 0.6s with a change in Q from 1000VAr to -750VAr. Such that, i_{abc} has been changed its peak value from 5.23A to 4.63A. The DC source side parameter values are continued without any variation as there is no change in V_{Bat} observed in Figure 9.

After 0.8 s, the converter acts as a PWM Inverter change its operation from Q_{IV} to Q_{III} with a change in P from 1000W to -2000W as well as change in Q from -750VAr to -500VAr. The response of the converter is shown in Figure 10. The peak of i_{abc} has been changed from 4.63A to 7.63A. The DC source current I_{L1} has been shifted to 10A with a change in P. A sudden shift in P caused a small voltage dip in V_{C3} and V_{DC} of the converter and restored within a single cycle. The

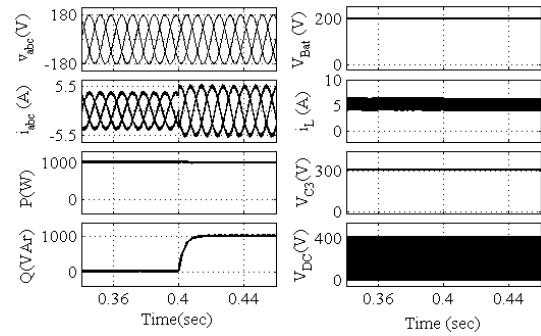


Figure 8. Response of IHTQZSC working in Q_I

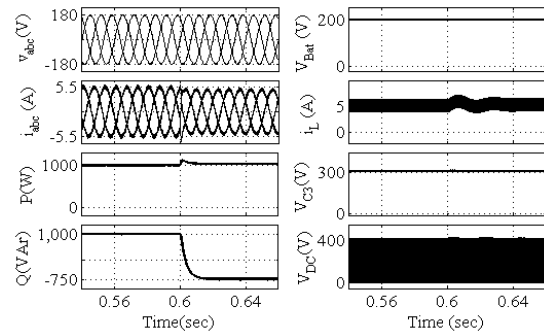


Figure 9. Response of IHTQZSC during Q_I to Q_{IV}

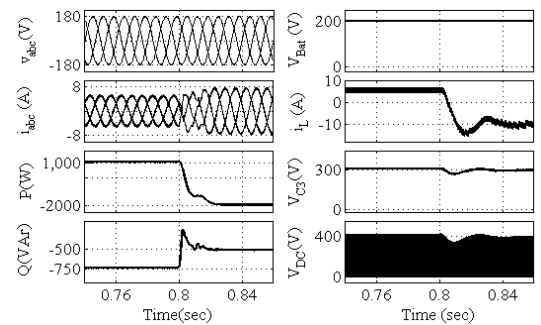


Figure 10. Response of IHTQZSC during Q_{IV} to Q_{III}

converter shifts its operation from Q_{III} to Q_{II} after 1 s due to a change in Q from -500VAr to 1200VAr. i_{abc} has been changed its peak value to 8.63A from 7.63A as shown in Figure 11. The DC source side parameters are continued, with constant V_{Bat} .

The transition of converter operation from Q_{II} to Q_I occurred at 1.2s observed in Figure 12, with the change in Q from 1200VAr to zero VAr. Simultaneously V_{Bat} has been reduced to 125V from 200V. With the change in V_{Bat} along with Q change, i_{abc} , i_{L1} , V_{C3} , and V_{DC} of the converter are disturbed for a period of three cycles and restored back to steady-state with the values at 7.4A, 10A, 281V and 438.2V, respectively. The impact of converter voltage gain and the power drawn from the converter on efficiency is shown in Figure 13.

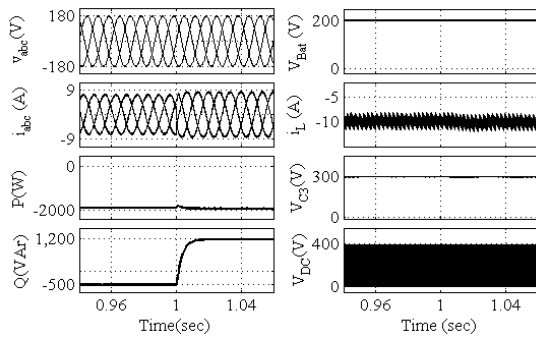


Figure 11. Response of IHTQZSC during QIII to QII

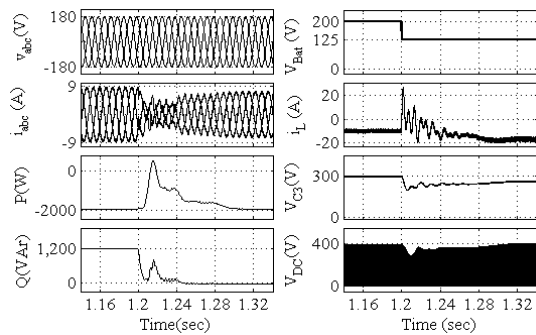


Figure 12. Response of IHTQZSC during QII to QI

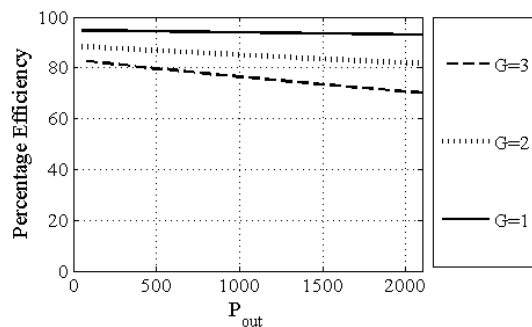


Figure 13. The efficiency variation of IHTQZSC

6. CONCLUSION

IHTQZSC ensures a wider range of voltage gain, among other high voltage gains ISC does not need any switching capacitors or charge pump cells. The voltage stress in the switching devices, capacitors, the current stress in the inductors and switching devices are deduced in this paper. The worthiness of the converter has been commended by comparing the voltage stress and current stress, peak SDP and power losses in the present converter with another high gain ISC. The converter has been working in all four quadrants, by injecting or consuming both active and reactive powers with the use of a predictive controller implemented for grid current tracking with a good dynamic response with the change

in dc source voltage as well as grid power. With the ability of bi-directional power control, high voltage gain, lower voltage stress and current stress in the converter elements with lesser peak SDP, the converter can be utilized in electric vehicles, energy storage systems, and in hybrid energy source systems.

7. REFERENCES

- Gobimohan, S., "Active power quality improvement for unified renewable energy system with multilevel inverter and peak controllers", *Energy Sources, Part A: Recovery, Utilization, and Environmental Effects*, Vol. 42, No. 21, (2020), 2603-2622. doi: 10.1080/15567036.2019.1612486.
- Ye, H., Jin, G., Fei, W. and Ghadimi, N., "High step-up interleaved dc/dc converter with high efficiency", *Energy Sources, Part A: Recovery, Utilization, and Environmental Effects*, (2020), 1-20. doi: 10.1080/15567036.2020.1716111.
- Ananthapadmanabha, B., Maurya, R. and Arya, S.R., "Improved power quality switched inductor cuk converter for battery charging applications", *IEEE Transactions on Power Electronics*, Vol. 33, No. 11, (2018), 9412-9423. doi: 10.1109/TPEL.2018.2797005.
- Gupta, J., Maurya, R. and Arya, S.R., "On-board electric vehicle battery charger with improved power quality and reduced switching stress", *IET Power Electronics*, Vol. 13, No. 13, (2020), 2885-2894. doi: 10.1049/iet-pel.2019.0962.
- Bhavya, K., Rama Rao, P. and Ravi Srinivas, L., "Performance evaluation of weighted feedback based upqc under various power quality issues", *International Journal of Engineering, Transactions C: Aspects*, Vol. 36, No. 3, (2023), 441-449. doi: 10.5829/ije.2023.36.03c.02.
- Tan, K.M., Padmanaban, S., Yong, J.Y. and Ramchandaramurthy, V.K., "A multi-control vehicle-to-grid charger with bi-directional active and reactive power capabilities for power grid support", *Energy*, Vol. 171, (2019), 1150-1163. doi: 10.1016/j.energy.2019.01.053.
- Chung, I.-Y., Liu, W., Schoder, K. and Cartes, D.A., "Integration of a bi-directional dc-dc converter model into a real-time system simulation of a shipboard medium voltage dc system", *Electric Power Systems Research*, Vol. 81, No. 4, (2011), 1051-1059. doi: 10.1109/ESTS.2009.4906531.
- Yong, J.Y., Ramchandaramurthy, V.K., Tan, K.M. and Selvaraj, J., "Experimental validation of a three-phase off-board electric vehicle charger with new power grid voltage control", *IEEE Transactions on Smart Grid*, Vol. 9, No. 4, (2016), 2703-2713. doi: 10.1109/TSG.2016.2617400.
- Tavassoli, F., Ghoreishy, H., Adabi, J. and Rezanejad, M., "An advanced modulation technique featuring common mode voltage suppression for three-phase neutral point clamped back to back converters", *International Journal of Engineering, Transactions B: Applications*, Vol. 35, No. 11, (2022), 2220-2228. doi: 10.5829/ije.2022.35.11b.17.
- Gadalla, B., Schaltz, E., Zhou, D. and Blaabjerg, F., "Lifetime prediction of boost, z-source and y-source converters in a fuel cell hybrid electric vehicle application", *Electric Power Components and Systems*, Vol. 46, No. 18, (2018), 1979-1991. doi: 10.1080/15325008.2018.1528316.
- Karimi, M., Mahdavi, M. and Torki Harchegani, A., "A new soft switching qzsc converter by using coupled inductor", *Electric Power Components and Systems*, Vol. 46, No. 3, (2018), 270-277. doi: 10.1080/15325008.2018.1444687.

12. Zhu, M., Yu, K. and Luo, F.L., "Switched inductor z-source inverter", *IEEE Transactions on Power Electronics*, Vol. 25, No. 8, (2010), 2150-2158. doi: 10.1109/TPEL.2010.2046676.
13. Nozadian, M.H.B., Babaei, E., Hosseini, S.H. and Asl, E.S., "Steady-state analysis and design considerations of high voltage gain switched z-source inverter with continuous input current", *IEEE Transactions on Industrial Electronics*, Vol. 64, No. 7, (2017), 5342-5350. doi: 10.1109/TIE.2017.2677315.
14. Jagan, V., Kotturu, J. and Das, S., "Enhanced-boost quasi-z-source inverters with two-switched impedance networks", *IEEE Transactions on Industrial Electronics*, Vol. 64, No. 9, (2017), 6885-6897. doi: 10.1109/TIE.2017.2688964.
15. Zhu, X., Zhang, B. and Qiu, D., "A new nonisolated quasi-z-source inverter with high voltage gain", *IEEE Journal of Emerging and Selected Topics in Power Electronics*, Vol. 7, No. 3, (2018), 2012-2028. doi: 10.1109/JESTPE.2018.2873805.
16. Shen, H., Zhang, B. and Qiu, D., "Hybrid z-source boost dc-dc converters", *IEEE Transactions on Industrial Electronics*, Vol. 64, No. 1, (2016), 310-319. doi: 10.1109/TIE.2016.2607688.
17. Kafle, Y.R., Hasan, S.U. and Town, G.E., "Quasi-z-source based bidirectional dc-dc converter and its control strategy", *Chinese Journal of Electrical Engineering*, Vol. 5, No. 1, (2019), 1-9. doi: 10.23919/CJEE.2019.0000001.
18. Hu, S., Liang, Z. and He, X., "Ultracapacitor-battery hybrid energy storage system based on the asymmetric bidirectional z-source topology for ev", *IEEE Transactions on Power Electronics*, Vol. 31, No. 11, (2015), 7489-7498. doi: 10.1109/TPEL.2015.2493528.
19. Vijayan, V. and Ashok, S., "High-performance bi-directional z-source inverter for locomotive drive application", *IET Electrical Systems in Transportation*, Vol. 5, No. 4, (2015), 166-174. doi: 10.1049/iet-est.2014.0053.
20. Siwakoti, Y.P., Peng, F.Z., Blaabjerg, F., Loh, P.C. and Town, G.E., "Impedance-source networks for electric power conversion part i: A topological review", *IEEE Transactions on Power Electronics*, Vol. 30, No. 2, (2014), 699-716. doi: 10.1109/TPEL.2014.2329859.
21. Ellabban, O., Van Mierlo, J. and Lataire, P., "A dsp-based dual-loop peak dc-link voltage control strategy of the z-source inverter", *IEEE Transactions on Power Electronics*, Vol. 27, No. 9, (2012), 4088-4097. doi: 10.1109/TPEL.2012.2189588.
22. Zhang, Y., Liu, Q., Gao, Y., Li, J. and Sumner, M., "Hybrid switched-capacitor/switched-quasi-z-source bidirectional dc-dc converter with a wide voltage gain range for hybrid energy sources evs", *IEEE Transactions on Industrial Electronics*, Vol. 66, No. 4, (2018), 2680-2690. doi: 10.1109/TIE.2018.2850020.
23. Kumar, A., Xiong, X., Pan, X., Reza, M., Beig, A.R. and Al Jaafari, K., "A wide voltage gain bidirectional dc-dc converter based on quasi-z-source and switched capacitor network", *IEEE Transactions on Circuits and Systems II: Express Briefs*, Vol. 68, No. 4, (2020), 1353-1357. doi: 10.1109/TCSII.2020.3033048.
24. Veerachary, M. and Kumar, P., "Analysis and design of quasi-z-source equivalent dc-dc boost converters", *IEEE Transactions on Industry Applications*, Vol. 56, No. 6, (2020), 6642-6656. doi: 10.1109/TIA.2020.3021372.
25. Zhang, Y., Fu, C., Sumner, M. and Wang, P., "A wide input-voltage range quasi-z-source boost dc-dc converter with high-voltage gain for fuel cell vehicles", *IEEE Transactions on Industrial Electronics*, Vol. 65, No. 6, (2017), 5201-5212. doi: 10.1109/TIE.2017.2745449.
26. Alla, R. and Chowdhury, A., "Csf-pc based grid tied improved hybrid three quasi z source converter", *COMPEL-The International Journal for Computation and Mathematics in Electrical and Electronic Engineering*, Vol. 39, No. 4, (2020), 927-942. doi: 10.1108/COMPEL-01-2020-0062.
27. Shen, M., Joseph, A., Wang, J., Peng, F.Z. and Adams, D.J., "Comparison of traditional inverters and z-source inverter for fuel cell vehicles", *IEEE Transactions on Power Electronics*, Vol. 22, No. 4, (2007), 1453-1463. doi: 10.1109/PET.2004.1393815.

COPYRIGHTS

©2023 The author(s). This is an open access article distributed under the terms of the Creative Commons Attribution (CC BY 4.0), which permits unrestricted use, distribution, and reproduction in any medium, as long as the original authors and source are cited. No permission is required from the authors or the publishers.

**Persian Abstract**

چکیده

مبدل‌های قدرت دو جهت برای مدیریت مؤثر انرژی الکتریکی موجود مرتبط با سیستم‌های انرژی تجدیدپذیر با استفاده از سیستم ذخیره‌سازی انرژی مورد استفاده قرار می‌گیرند. مبدل هیبریدی سه شبه منبع (IHTQZSC) در این مقاله پیشنهاد شده است که افزایش ولتاژ بالاتری را بدون هیچ خازن سوئیچ یا سلول پمپ شارژ ارائه می‌دهد. در این مقاله IHTQZSC برای کاربردهای انتقال قدرت و کنترل دو جهت در نظر گرفته شده است. مبدل افزایش ولتاژ گسترده ای را در یک سیستم تبدیل توان $DC \leftrightarrow AC$ تک مرحله ای با لحظه‌های تیراندازی کمتر تضمین می‌کند. صلاحیت مبدل با تنش ولتاژ، تنش جریان، توان دستگاه سوئیچینگ پیک و تلفات توان در مقایسه با دیگر مبدل‌های افزایش ولتاژ بالا تحسین شده است. تأثیر افزایش ولتاژ و توان گرفته شده توسط مبدل بر بازده توضیح داده شده است. کنترل توان چهار ربعی با کنترل کننده پیش بینی فرکانس سوئیچینگ ثابت به دست می‌آید. ولتاژ DC-link مبدل با یک کنترل کننده PI کنترل می‌شود و یک کنترل کننده پیش بینی برای ردیابی جریان شبکه استفاده می‌شود. کار دو طرفه مبدل با نرم افزار MATLAB/Simulink نشان داده شده است.